



Synthesis and biological evaluation of novel pyridine derivatives as potential anticancer agents and phosphodiesterase-3 inhibitors



Atieh Sadat Davari^a, Khalil Abnous^b, Soghra Mehri^c, Morteza Ghandadi^d, Farzin Hadizadeh^{d,*}

^a Student Research Committee, School of Pharmacy, Mashhad University of Medical Sciences, Mashhad, Iran

^b Pharmaceutical Research Center, School of Pharmacy, Mashhad University of Medical Sciences, Mashhad, Iran

^c Pharmaceutical Research Center, Department of Pharmacodynamics and Toxicology, School of Pharmacy, Mashhad University of Medical Sciences, Mashhad, Iran

^d Biotechnology Research Center, School of Pharmacy, Mashhad University of Medical Sciences, Mashhad, Iran

ARTICLE INFO

Article history:

Received 17 March 2014

Available online 17 September 2014

Keywords:

Phosphodiesterase

Inhibition

Anticancer

Synthesis

ABSTRACT

Phosphodiesterases (PDEs) have been studied in a variety of tumours; data have suggested that the levels of PDE activities are elevated and, therefore, the ratios of cGMP to cAMP are affected. In addition, PDE inhibitors are potential targets for tumour cell growth inhibition and induction of apoptosis. Nonselective PDE inhibitors, such as theophylline or aminophylline, are known regulators of growth in a variety of carcinoma cell lines, suggesting a potential role for PDE inhibitors as anticancer drugs.

In the current study, we reported the synthesis of novel derivatives of 6-aryl-4-imidazolyl-2-imino-1,2-dihydropyridine-3-carbonitriles (Ia,b,c) and their 2-oxo isosteres (IIa,b,c,d). All the compounds were evaluated for their PDE3A inhibitory effects, as well as their cytotoxic effects on MCF-7 and HeLa cell lines. Moreover, structure–activity relationships were studied.

4-(1-benzyl-2-ethylthio-5-imidazolyl)-6-(4-bromophenyl)-2-imino-1,2-dihydropyridine-3-carbonitrile (Ib) exhibited the strongest PDE3A inhibitory effects with an IC_{50} of 3.76 ± 1.03 nM. Compound Ib also showed the strongest cytotoxic effects on both the HeLa and MCF-7 cells with an IC_{50} of 34.3 ± 2.6 μ M and 50.18 ± 1.11 μ M, respectively. There was a direct correlation between PDE3 inhibition and anticancer activity for the synthesised compounds.

The data reported here support our view that PDEs represent promising cellular targets for antitumor treatment.

© 2014 Elsevier Inc. All rights reserved.

1. Introduction

Eleven cyclic nucleotide phosphodiesterase gene families (PDE1–11) have been identified in various tissues or cells. PDEs are characterised based on their primary amino acid sequences, their affinities for cAMP and cGMP, their sensitivities to specific inhibitors, their biochemical and physical properties and their biological regulatory pathways [1–11]. PDE isoforms can influence disease pathogenesis and be novel therapeutic targets [12]. Impaired cAMP and/or cGMP generation upon overexpression of PDE isoforms have been described in various cancer pathologies [13].

Selective inhibition of PDE isoforms, which raises the levels of intracellular cAMP and/or cGMP, may regulate the tumour micro-environment and induce apoptosis and cell cycle arrest in a broad spectrum of tumour cells. Therefore, development and clinical

application of inhibitors specific for individual PDE isoenzymes may selectively restore normal intracellular signalling and provide antitumour therapy with reduced adverse effects [14,15]. PDE3 isoforms are found in a variety of tissues, including myocardium, platelets and adipose tissue [1–3]. Two PDE3 genes, PDE3A and PDE3B have been discovered in humans and these genes are located on human chromosomes 11 and 12, respectively [16]. Studies on specific PDE3 inhibitors suggest that PDE3s are important in the regulation of cAMP-modulated processes, including myocardial contractility, platelet aggregation and antiproliferative action [1–3].

Recent studies have shown that PDE3, PDE4 and PDE5 are over-expressed in cancer cells. In addition, inhibition of PDE3 along with other PDEs may lead to inhibition of tumour cell growth and angiogenesis [17–21].

In this study, we reported the synthesis of novel derivatives of 6-aryl-4-imidazolyl-2-imino-1,2-dihydropyridine-3-carbonitriles (I) and their 2-oxo isosteres (II). The PDE3A inhibitory effects, as well as the cytotoxic effects, of synthesised compounds on

* Corresponding author. Fax: +98 51 38823251.

E-mail address: hadizadehf@mums.ac.ir (F. Hadizadeh).

MCF-7 and HeLa cell lines were evaluated. Moreover, structure–activity relationships were studied.

2. Results and discussion

For many cancers, there has been a shift from management with traditional, nonspecific cytotoxic chemotherapies to treatment with molecule-specific targeted therapies that are used either alone or in combination with traditional chemotherapies [22,23] here, we designed and synthesised some new PDE3A inhibitors. The cytotoxicity and PDE3A inhibitory effect of these compounds were evaluated both in the lab and in silico.

2.1. Chemistry

The general synthesis of 6-aryl-4-imidazolyl-2-imino-1,2-dihydropyridine-3-carbonitriles (Ia–c) and 6-aryl-4-imidazolyl-2-oxo-1,2-dihydropyridine-3-carbonitriles (IIa–d) is illustrated in Fig. 1. Briefly, 4-bromoacetophenone or 1-(1,3-benzodioxol-5-yl) ethanone were reacted with the appropriate aldehyde, namely 2-alkyl thio-1-benzyl-5-formyl imidazolyl, in the presence of malononitrile or ethyl cyanoacetate and ammonium acetate. The infrared (IR) spectra of all derivatives showed bands at a stretching frequency (m) around 3400 cm^{-1} corresponding to the NH, which showed relatively lower values of the carbonyl with a stretching frequency (m) around 1632 cm^{-1} .

2.2. Biology

The cytotoxic effects of synthesised compounds on HeLa and MCF-7 cell lines were determined using MTT assay. PDE3A activity was analysed using an IMAP TR-FRET phosphodiesterase assay kit and cAMP as the substrate. As shown in Fig. 2, there was a direct correlation between PDE3 inhibition and cytotoxic activities of the synthesised compounds ($r^2 = 0.89$). 4-(1-benzyl-ethylthio-5-imidazolyl)-6-(4-bromophenyl)-2-imino-1,2-dihydropyridine-3-carbonitrile (Ib) exhibited the strongest PDE3A inhibition ($\text{IC}_{50} = 3.76 \pm 1.03\text{ nM}$). Compound Ib was also the most cytotoxic compound against both the HeLa and MCF-7 tumour cells, as the IC_{50} values were measured to be $34.3 \pm 2.6\text{ }\mu\text{M}$ and $50.18 \pm 1.11\text{ }\mu\text{M}$, respectively. The electronic and steric effects, as well as the H-bond capabilities of the synthesised compounds, were all crucial in PDE3 inhibition and cytotoxicity. Our data are summarised in Table 1.

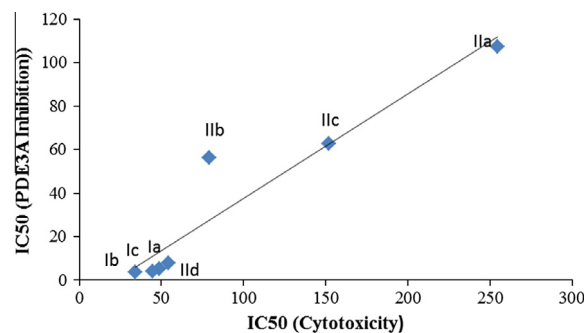


Fig. 2. Correlation between PDE3 inhibition and cytotoxic activities of synthesized compounds on HeLa cell line.

The data summarised here may support our view that PDEs represent promising cellular targets for antitumour treatment (Table 1).

For investigating the structure–activity relationship, different substitutes are compared according to the potency of the compounds. As demonstrated, all the compounds in the imino group have shown higher IC_{50} s than the chemicals with the oxo substitute. In addition, a comparison of IIc with IIa and IIb with IId in the oxo group and Ic with Ia in imino group demonstrated that a benzodioxol substitute can make chemicals more potent than a bromobenzene group. On the other hand, compound Ib is more potent than compound Ia, and compounds IIb and IId are more potent than compounds IIa and IIc, respectively. This proves that the SET group is better than the SMe group in PDEs inhibition. In conclusion, chemicals with imino, benzodioxol and SET groups are more potent than compounds with oxo, bromobenzene and SMe groups.

2.3. Docking

The accuracy of the docking procedure was examined by calculating the correlation between theoretical k_i and the experimental IC_{50} of the compounds. A high correlation between k_i and IC_{50} values has been considered to be evidence of the validity of the docking procedure (Figs. 3–5). On the other hand, the IC_{50} values of compounds were in micromolar range whereas theoretical k_i values were in nanomolar range. Really several approximations have been made in theoretical K_i calculation and in real in vitro experiment several factors like low cell permeability; removal by ABC exporters and metabolism by cells may be involved.

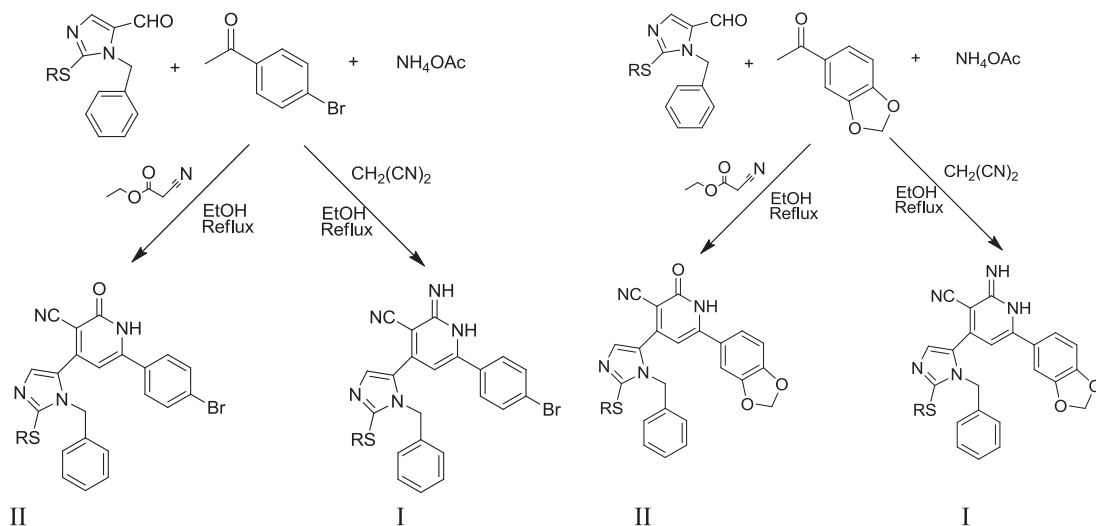
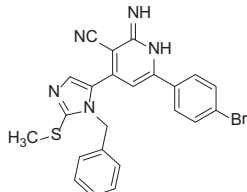
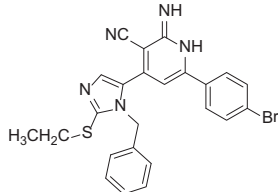
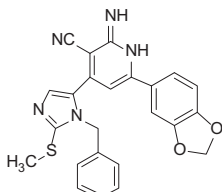
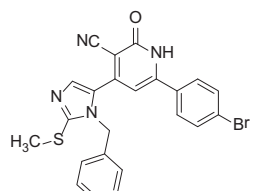
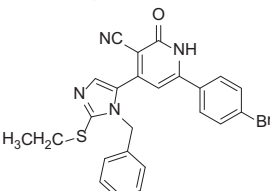
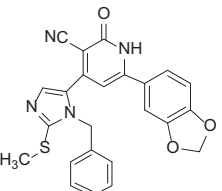
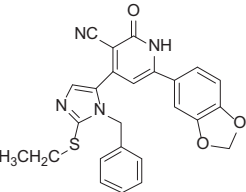
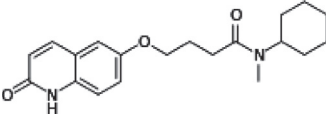


Fig. 1. Synthesis of 4-imidazolyl-6-aryl-2-imino-1,2-dihydropyridine-3-carbonitriles (Ia,b,c) and their 2-oxo isosteres (IIa,b,c,d).

Table 1

Inhibitory effect of the synthesized compounds on Hela and MCF-7 cells and PDE3.

Compounds	Growth inhibition IC ₅₀ (μM) ± SEM		PDE3 inhibition IC ₅₀ (nM) ± SEM	Ki (μM) in silico
	Hela	MCF-7		
 Ia	48.72 ± 2.12	77.06 ± 6.01	5.04 ± 1.27	75
 Ib	34.3 ± 2.6	50.18 ± 1.11	3.76 ± 1.03	40.06
 Ic	44.58 ± 4.12	62.57 ± 2.01	3.97 ± 0.46	50.36
 IIa	254.7 ± 1.1	322 ± 5	107.4 ± 3.7	282
 IIb	79.12 ± 3.03	106.1 ± 4.1	56.35 ± 0.78	76.41
 IIc	152.18 ± 2.12	207.6 ± 3.4	62.64 ± 0.86	95.72
 IIId	54.19 ± 5.41	96.52 ± 1.21	7.96 ± 0.25	61.12
 Cilostamide	ND*	ND	63.98 ± 0.57	173.97

* Not determined

The binding cavity, which is identified by superimposing 30 top score poses in protein, is represented in Fig. 6. As shown, the Ia compound poses are represented in a stick fashion while the

protein structure is represented as a line. Fig. 7 shows seven synthesised compounds in the middle of the binding cavity, which demonstrates appropriate interactions among the ligands and the

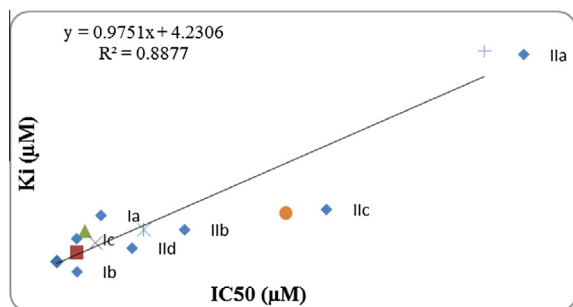


Fig. 3. Correlation between theoretical K_i and experimental IC_{50} in Hela cells.

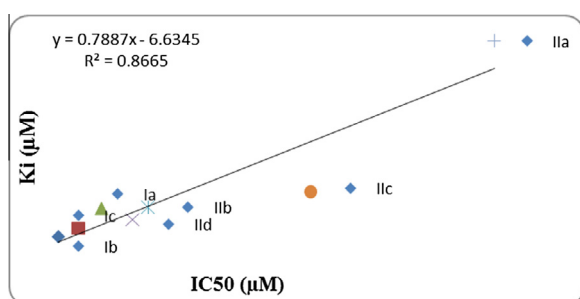


Fig. 4. Correlation between theoretical K_i and experimental IC_{50} in MCF-7 cells.

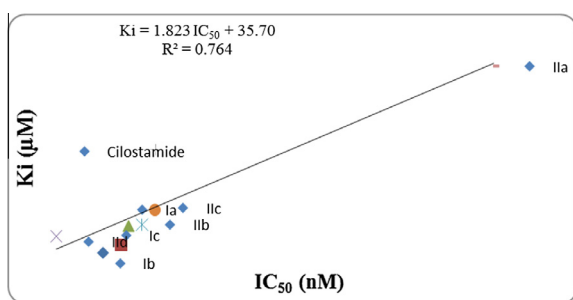


Fig. 5. Correlation between theoretical K_i and experimental IC_{50} of PDE3.

protein. It was mentioned above a benzodioxol substitute can make chemicals more potent than a bromobenzene group (Table 1). As Fig. 8 shows, there are a few greasy amino acids, like Phe193, Phe161, Phe178 and Leu99, near the benzodioxol group at the binding site, so this can create an opportunity for hydrophobic interactions and it can provide an explanation for the powerful cytotoxicity of compounds with a benzodioxol substitute (Fig. 8); on the other hand, the hydrogen bonds between substitutes in the pyridine ring and in amino acids, like Gln190, Thr154 and Gly142, are examples of other important interactions found in these inhibitors (albeit Gln190 is a key residue in hydrogen bond formation, because all the represented compounds have at least one hydrogen bond through this residue). Fig. 9 shows an example of a 2D graph of ligand-receptor interactions of four synthesised chemicals; other compounds have shown the same interactions.

3. Conclusion

In conclusion, a high correlation between IC_{50} cytotoxicity and IC_{50} PDE3A inhibition (Fig. 2) may support the idea that proposes PDE3 inhibitors as cytotoxic chemicals. In addition, according to docking and SAR investigations, hydrophobic interactions are as

important as hydrogen bond formation for cytotoxic effects and PDE3 inhibition of these compounds.

4. Experimental procedure

4.1. Chemistry

Melting points were determined using an Electrothermal Capillary apparatus and are uncorrected. The 1H NMR spectra were recorded on a Bruker spectrometer at 100 MHz using tetramethylsilane (TMS) as an internal reference. Chemical shift values were given in ppm, at room temperature using DMSO- d_6 as a solvent; chemical shifts (δ) were reported in parts per million (ppm) down-field from TMS; multiplicities were abbreviated as: s: singlet; d: doublet; q: quartet; m: multiplet; dd: doublet of doublet; br s: broad singlet. ^{13}C NMR spectra were recorded at 25 MHz. Errors of elemental analyses were within $\pm 0.4\%$ of theoretical values. IR spectra were recorded on a Perkin-Elmer Paragon 1000 spectrophotometer. The yields were not optimised.

4.1.1. The general procedure for the preparation of 6-(4-bromophenyl)-4-imidazolyl-2-imino-1,2-dihydropyridines-3-carbonitriles and 6-(1,3-benzodioxol-5-yl)-4-imidazolyl-2-imino-1,2-dihydropyridines-3-carbonitriles (Ia–c)

A mixture of p-bromoacetophenone or 3,4-methylenedioxyacetophenone (2.5 mmol), appropriate aldehyde (2.5 mmol), malononitrile (0.16 g, 2.5 mmol) and ammonium acetate (1.54 g, 20 mmol) in ethanol (50 ml) was heated under reflux for 18–24 h. The reaction mixture was cooled and the formed precipitate was filtered, washed with ethanol, then washed successively with water, dried and crystallized from DMF/ethanol 1:2, respectively.

4.1.1.1. 4-(1-benzyl-2-(methylthio)-1H-imidazol-5-yl)-6-(4-bromophenyl)-2-imino-1,2-dihydropyridine-3-carbonitrile (Ia). Yield: 42.28%; mp 235–238 °C; IR (KBr): 3450.22, 2216.89($C\equiv N$), 1600.12 cm^{-1} ; 1H NMR (DMSO- d_6): δ 8–6.6 (m, 12H, aromatic, H–C₄imidazole, NH) 5 (s, 2H, CH_2N), 2.4 ppm (s, 3H, SCH_3). ^{13}C NMR (DMSO- d_6): δ 164.41, 154.33, 139.20, 137.29, 137.01, 135.69, 133.19, 131.73, 131.73, 128.76, 128.76, 128.53, 128.53, 128.43, 128.43, 128.01, 127.55, 124.25, 112.02, 104.72, 93.88, 50.18, 14.50. Anal. Calcd for $C_{23}H_{18}BrN_5S$: C, 57.99; H, 3.81; N, 14.70. Found: C, 58.20; H, 3.80; N, 14.65.

4.1.1.2. 4-(1-benzyl-ethylthio-5-imidazolyl)-6-(4-bromophenyl)-2-imino-1,2-dihydropyridine-3-carbonitrile (Ib). Yield: 50.15%; mp 210–214 °C; IR (KBr): 3458.25, 2216.89($C\equiv N$), 1600.13 cm^{-1} ; 1H NMR (DMSO- d_6): δ 7.4–6.3 (m, 12H, aromatic, H–C₄imidazole, NH) 5 (s, 2H, CH_2N), 2.2 (q, 2H, CH_2S), 1 ppm (t, 3H, CH_3). ^{13}C NMR (DMSO- d_6): δ 164.41, 157.25, 139.20, 137.29, 137.01, 135.69, 133.19, 131.73, 131.73, 128.76, 128.76, 128.53, 128.53, 128.43, 128.43, 128.01, 127.55, 124.25, 112.02, 104.72, 93.88, 50.18, 26.98, 13.97. Anal. Calcd for $C_{24}H_{20}BrN_5S$: C, 58.78; H, 4.11; N, 14.28. Found: C, 58.76; H, 4.12; N, 14.22.

4.1.1.3. 4-(1-benzyl-methylthio-5-imidazolyl)-6-(1,3-benzodioxol-5-yl)-2-imino-1,2-dihydropyridines-3-carbonitriles (Ic). Yield: 37.11%; mp 197–200 °C; IR (KBr): 3450.11, 2215.09($C\equiv N$), 1595.24 cm^{-1} ; 1H NMR (DMSO- d_6): δ 7.2–6.8 (m, 11H, aromatic, H–C₄imidazole, NH), 5.82 (s, 2H, OCH_2O), 5 (s, 2H, CH_2N), 2.2 ppm (s, 3H, SCH_3). ^{13}C NMR (DMSO- d_6): δ 164.41, 154.33, 149.98, 149.40, 139.20, 137.01, 135.69, 135.46, 129.80, 128.76, 128.76, 128.53, 128.53, 128.01, 127.55, 122.56, 112.02, 107.49, 107.18, 105.02, 102.12, 93.88, 50.18, 14.50. Anal. Calcd for $C_{24}H_{19}N_5O_2S$: C, 65.29; H, 4.34; N, 15.86. Found: C, 65.38; H, 4.33; N, 15.90.

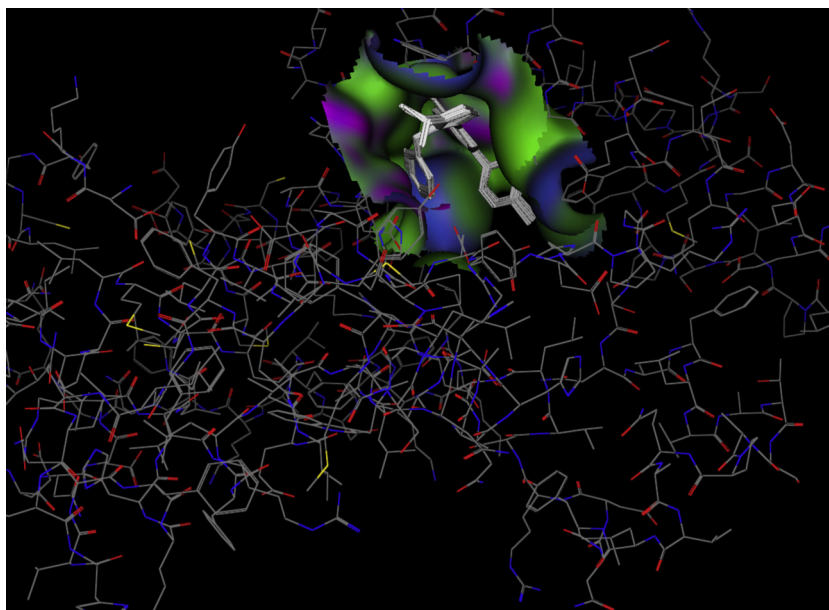


Fig. 6. 30 Top score poses of docked 1a compound superimposed into the PDE3A homology model (PDB ID: 1LRC) to find binding cavity of these inhibitors (Poses are shown in stick and coloured by atom, protein is drawn by line and coloured by atom).

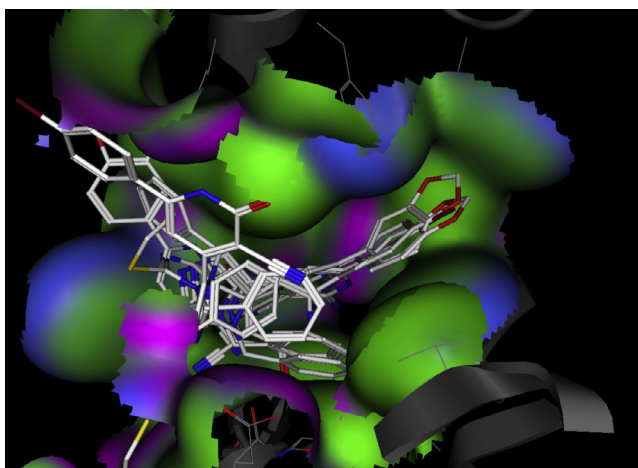


Fig. 7. Seven docked compounds superimposed in binding cavity of PDE3A. Compounds represent as line and coloured by atom. Green hydrophobic, violet H-bond and blue as middle polar represent electrostatic map of binding cavity.

4.1.2. The general procedure for the preparation of 6-(4-bromophenyl)-4-imidazolyl-2-oxo-1,2-dihydropyridin-3-carbonitriles and 6-(1,3-benzodioxol-5-yl)-4-imidazolyl-2-oxo-1,2-dihydropyridin-3-carbonitriles (IIa–d)

A mixture of p-bromoacetophenone or 3,4-methylenedioxyacetophenone (2.5 mmol), appropriate aldehyde (2.5 mmol), ethyl cyanoacetate (0.28 g, 2.5 mmol) and ammonium acetate (1.54 g, 20 mmol) in ethanol (50 ml) was heated under reflux for 10–20 h. The reaction mixture was cooled and the formed precipitate was filtered, washed with ethanol, then washed successively with water, dried and crystallized from DMF/ethanol 1:2, respectively.

4.1.2.1. 4-(1-benzyl-methylthio-5-imidazolyl)-6-(4-bromophenyl)-2-oxo-1,2-dihydropyridine-3-carbonitrile (IIa). Yield: 31.93%; mp 280–283 °C; IR (KBr): 3483.45, 2215.84 (C≡N), 1642.49 cm⁻¹; ¹H NMR (DMSO-d₆): δ 8–6.6 (m, 11H, aromatic, H–C₄imidazole, NH), 5 (s, 2H, CH₂N), 2.4 ppm (s, 3H, SCH₃). ¹³C NMR (DMSO-d₆) δ 163.61, 154.33, 143.51, 141.46, 137.01, 135.69, 133.19, 131.73, 131.73, 128.76, 128.76, 128.53, 128.53, 128.43, 128.43, 128.01, 127.55,

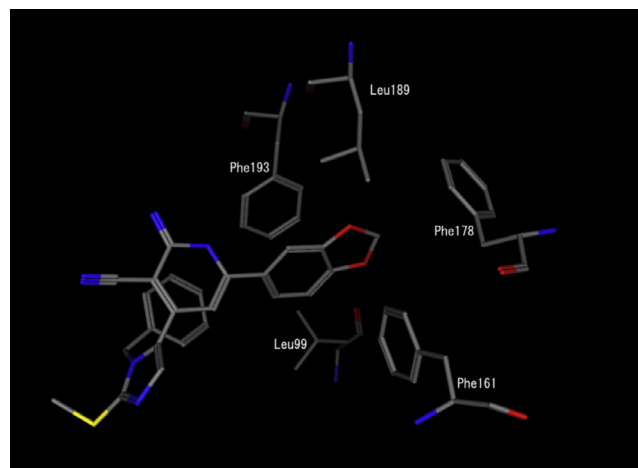


Fig. 8. 3D structure of docked compound 1c and position of five greasy amino acids close to benzodioxol substitute (other residues and hydrogens were hidden for clarification).

124.25, 111.21, 103.33, 103.22, 50.18, 14.50. Anal. Calcd for C₂₃H₁₇BrN₄OS: C, 57.87; H, 3.59; N, 11.74. Found: C, 58.07; H, 3.58; N, 11.70.

4.1.2.2. 4-(1-benzyl-ethylthio-5-imidazolyl)-6-(4-bromophenyl)-2-oxo-1,2-dihydropyridine-3-carbonitrile (IIb). Yield: 48.02%; mp 287–291 °C; IR (KBr): 3475.33, 2215.84 (C≡N), 1642.49 cm⁻¹; ¹H NMR (DMSO-d₆): δ 7.4–6.3 (m, 11H, aromatic, H–C₄imidazole, NH), 5 (s, 2H, CH₂N), 2.2 (q, 2H, CH₂S), 1 ppm (t, 3H, SCH₃). ¹³C NMR (DMSO-d₆) δ 163.61, 157.25, 143.51, 141.46, 137.01, 135.69, 133.19, 131.73, 131.73, 128.76, 128.76, 128.53, 128.53, 128.43, 128.43, 128.01, 127.55, 124.25, 111.21, 103.33, 103.22, 50.18, 26.98, 13.97. Anal. Calcd for C₂₄H₁₉BrN₄OS: C, 58.66; H, 3.90; N, 11.40. Found: C, 58.45; H, 3.88; N, 11.35.

4.1.2.3. 4-(1-benzyl-methylthio-5-imidazolyl)-6-(1,3-benzodioxol-5-yl)-2-oxo-1,2-dihydropyridine-3-carbonitriles (IIc). Yield: 41.17%; mp 258–260 °C; IR (KBr): 3451.81, 2217.49 (C≡N), 1632.48 cm⁻¹; ¹H NMR (DMSO-d₆): δ 7.44–6.44 (m, 10H, aromatic,

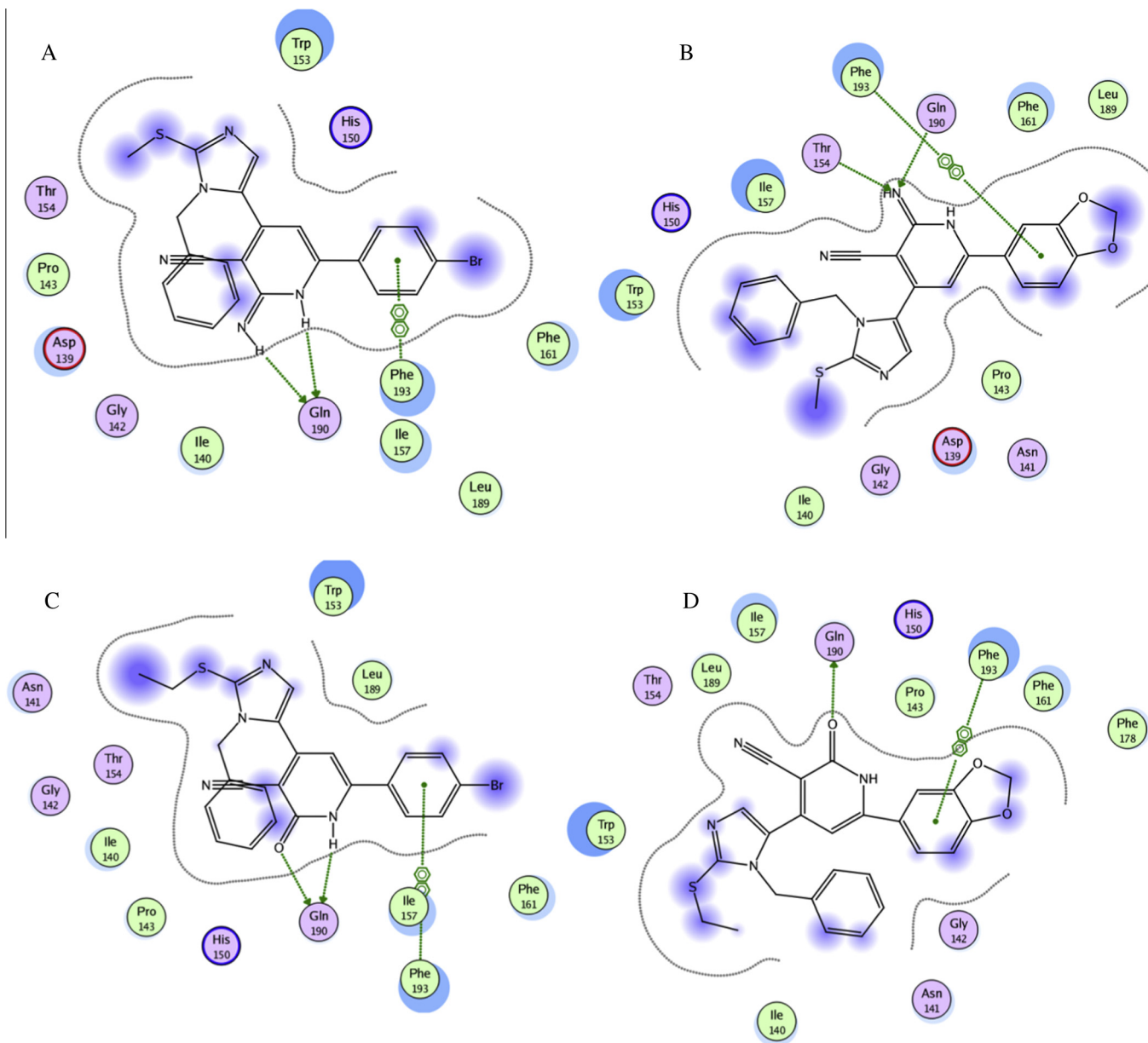


Fig. 9. 2D graphs of interactions between compound Ia (A), Ic (B), Ilb (C) and Ild (D) and PDE3A enzyme (PDB ID: 1LRC). Graphs are made using MOE software. In this plots hydrophobic/aromatic residues are coloured in green, whereas polar amino acids in magenta. H bonds and all π stacking interactions are shown as green dotted lines. The active site contour is also shown.

H—C₄imidazole, NH), 5.82 (s, 2H, OCH₂O), 5 (s, 2H, CH₂N), 2.4 ppm (s, 3H, SCH₃). ¹³C NMR (DMSO-d₆): δ 163.61, 154.33, 149.98, 149.40, 141.46, 140.99, 137.01, 135.69, 129.80, 128.76, 128.76, 128.53, 128.53, 128.01, 127.55, 122.56, 111.21, 107.49, 107.18, 104.82, 103.22, 102.12, 50.18, 14.50. Anal. Calcd for C₂₄H₁₈N₄O₃S: C, 65.14; H, 4.10; N, 12.66. Found: C, 64.88; H, 4.08; N, 12.60.

4.1.2.4. 4-(1-benzyl-ethylthio-5-imidazolyl)-6(1,3-benzodioxol-5-yl)-2-oxo-1,2-dihydropyrid-ines-3-carbonitriles (Ild). Yield: 47.94%; mp 250–252 °C; IR (KBr): 3481.43, 2217.49 (C≡N), 1632.48 cm⁻¹; ¹H NMR (DMSO-d₆): δ 7.44–6.44 (m, 10H, aromatic, H—C₄imidazole—NH), 5.82 (s, 2H, OCH₂O), 5 (s, 2H, CH₂N), 2.8 (q, 2H, CH₂S), 1 ppm (t, 3H, SCH₃). ¹³C NMR (DMSO-d₆): δ = 163.61, 157.25, 149.98, 149.40, 141.46, 140.99, 137.01, 135.69, 129.80, 128.76, 128.76, 128.53, 128.53, 128.01, 127.55, 122.56, 111.21, 107.49, 107.18, 104.82, 103.22, 102.12, 50.18, 26.98, 13.97. Anal. Calcd

for C₂₅H₂₀N₄O₃S: C, 65.77; H, 4.42; N, 12.27. Found: C, 65.01; H, 4.43; N, 12.22.

4.2. Biology

4.2.1. Phosphodiesterase 3A activity assay

An IMAP TR-FRET phosphodiesterase assay kit was used to determine PDE3 activity. This assay was based on hydrolysis of a diester bond in fluorescein-labelled cAMP by PDE3. Both AMP-fluorescein and Phospho-Tb-Donor then bind to the immobilised metal (MIII) coordination complexes on the nanoparticles (IMAP). This type of binding brings the fluorophore and the nucleotide mono phosphate in close proximity to the Tb-Donor so that Fluorescence Resonance Energy Transfer (FRET) is generated upon excitation of FAM. Due to the long lifetime of the Tb-Donor, fluorescence intensities can be measured in a time-resolved mode, which further reduces the background fluorescence created by the cell

components. Briefly, 10 μ L of diluted phosphodiesterase 3A human (E8784 Sigma) enzyme and 10 μ L of the substrate solution, prepared by adding 3 μ L of the 100 μ M cAMP substrate solution per 1500 μ L of complete reaction buffer, were mixed in each of the microplate wells. For the buffer-only control and the Tb-only control, 10 μ L of enzyme dilution buffer and 10 μ L complete reaction buffer were added to the assigned wells. Then, the plate was incubated at room temperature for 60 min.

Then 60 μ L IMAP binding solution, containing 70% binding buffer A, 30% binding buffer B and binding reagent 1:800, and Tb-Donor 1:400 (all of these reagents were provided in the kit) were added to all the wells, including the “Tb-only control” wells. Then, 60 μ L of binding solution without Tb-Donor was added to the “buffer-only control” wells. The plate was then incubated at room temperature for 3 h. Finally the fluorescence intensities were determined according to the appropriate wavelength for Tb intensities and TR-FRET using Synergy H4 Hybrid Multi-Mode Microplate Reader (BioTek, Model: H4MLFPTAD).

The corrected FRET ratio, which has a direct correlation with PDE activity, was calculated using Eq. (1), as follows:

$$\text{Corrected FRET ratio} = \frac{(\text{FRET}_{\text{sample}} - (P \times \text{Sample 490}))}{\text{Sample 490}} \times 10000 \quad (1)$$

where $\text{FRET}_{\text{sample}}$ = RFU at 520 nm in one assay well, minus average RFU at 520 nm in the buffer-only control, Sample 490 = RFU at 490 nm in one assay well, minus average RFU at 490 nm in the buffer-only control, P (a correction coefficient for Tb-Donor contribution to the FRET signal = $\text{Tb520}/\text{Tb490}$), Tb520 = average RFU at 520 nm in the Terbium-only control, minus average RFU at 520 nm in the buffer-only control and Tb490 = RFU at 490 nm in the Terbium-only control minus RFU at 490 nm in the buffer-only control.

4.2.2. Experiments in cell cultures

The HeLa and MCF-7 cell lines were obtained from the National Cell Bank of Iran, Pasteur Institute of Iran. The cells were cultured in DMEM medium supplemented with 10% (v/v) heat-inactivated foetal bovine serum, 100 U/ml penicillin and 100 mg/ml streptomycin, at 37 °C in a humidified atmosphere (95%) containing 5% CO_2 .

To determine the cytotoxic effects of the synthesised compounds, an MTT [3-(4,5-Dimethylthiazol-2-yl)-2,5-diphenyltetrazolium bromide] assay was performed [24,25]. Briefly, 5000 HeLa cells/wells or 10,000 MCF-7 cells/wells were seeded in a 96-well plate and cultured overnight. (0, 6.25, 12.5, 25, 50, 100 and 200 μ M) concentrations of the synthesised compounds were added to each well. After incubation for 24 h, the cells were treated with a final concentration of 0.5 mg/ml MTT solution for 4 h at 37 °C. Then, the medium was removed, and the purple formazan crystals were dissolved in 150 μ L dimethylsulfoxide (DMSO). Absorbance was measured at 545 nm (630 nm as a reference) in a Synergy H4 Hybrid Multi-Mode Microplate Reader (BioTek, USA). IC_{50} was calculated using Prism 5.0 software (<http://www.graphpad.com/scientific-software/prism/>).

4.3. Docking

The mode of interaction between the compounds and PDE3 was investigated by docking. A 3D structure of the chemicals was prepared using Hyperchem 7 software (<http://www.hyper.com/>), using the AM1 semi-empirical calculation following molecular mechanic force field pre-optimisation. The PDE3A theoretical

homology model was downloaded from the protein data bank (PDB ID: 1LRC), opened in an AutoDock tools version 1.5.4 program (<http://mgltools.scripps.edu/>) and prepared for docking after adding polar hydrogens. At first, docking was run using a whole protein as the binding site and the compound 1a as the ligand in the AutoDock 4.0 software (<http://autodock.scripps.edu>) to identify the binding pocket. Thirty top score poses, between 100 retained structures, were superimposed in the protein and the docking box was adjusted around the structures, then all the compounds were docked into the identified binding cavity of the PDE3A protein. Theoretical k_i was calculated by analysing the docking results using the AutoDock tools and the ligand–protein interactions pictures were created using MOE 2008.10 software (<http://www.chemcomp.com/>).

Conflict of interest

The authors confirm that there is no conflict of interest.

Acknowledgment

The authors gratefully acknowledge the Vice Chancellor of Research, Mashhad University of Medical Sciences for financial support. The results described in this paper are part of a PharmD thesis.

References

- [1] V.C. Manganiello, T. Murata, M. Taira, P. Belfrage, E. Degerman, Arch. Biochem. Biophys. 322 (1995) 1–13.
- [2] V.C. Manganiello, M. Taira, E. Degerman, P. Belfrage, Cell Signal. 7 (1995) 445–455.
- [3] E. Degerman, P. Belfrage, V.C. Manganiello, J. Biol. Chem. 272 (1997) 6823–6826.
- [4] E. Meacci, M. Taira, M. Moos, Proc. Natl. Acad. Sci. USA 89 (1992) 3721–3725.
- [5] M. Taira, S.C. Hockman, J.C. Calvo, M. Taira, P. Belfrage, V.C. Manganiello, J. Biol. Chem. 268 (1993) 18573–18579.
- [6] D.A. Fisher, J.F. Smith, J.S. Pillar, S.H. Denis, J.B. Cheng, Biochem. Biophys. Res. Commun. 246 (1998) 570–577.
- [7] M. Hayashi, K. Matsushima, H. Ohashi, Biochem. Biophys. Res. Commun. 250 (1998) 751–756.
- [8] S.H. Soderling, S.J. Bayuga, J.A. Beavo, Proc. Natl. Acad. Sci. USA 95 (1998) 8991–8996.
- [9] D.A. Fisher, J.F. Smith, J.S. Pillar, S.H. Denis, J.B. Cheng, J. Biol. Chem. 273 (1998) 15559–15564.
- [10] K. Fujishige, J. Kotera, H.J. Michibata, Biol. Chem. 274 (1999) 18438–18445.
- [11] L. Fawcett, R. Baxendale, P. Stacey, Proc. Natl. Acad. Sci. USA 97 (2000) 3702–3707.
- [12] L. Zhanga, F. Murraya, A. Zahnoa, J.A. Kantera, D. Choua, R. Suda, M. Fenlonb, L. Rassentib, H. Cottamb, T.J. Kippseb, Proc. Natl. Acad. Sci. USA 105 (2008) 19532–19537.
- [13] K. Omori, J. Kotera, Circ. Res. 100 (2007) 309–327.
- [14] R. Savai, S.S. Pullamsetti, G.A. Banat, N. Weissmann, H.A. Ghofrani, F. Grimminger, R.T. Schermuly, Expert. Opin. Invest. Drugs. 1 (2010) 117–131.
- [15] Y. Shakur, L.S. Holst, T.R. Landstrom, M. Movsesian, E. Degerman, V. Manganiello, Prog. Nucleic. Acid. Res. Mol. Biol. 66 (2001) 241–277.
- [16] V.C. Manganiello, E. Degerman, Thromb. Haemost. 82 (1999) 407–411.
- [17] P. Gary, J.W. Soh, Y. Mao, M.G. Kim, R. Pamukcu, H. Li, W.J. Thompson, I.B. Weinstein, Clin. Cancer Res. 6 (2000) 4136–4141.
- [18] J. Cheng, J.P. Grande, Exp. Biol. Med. 232 (2007) 38–51.
- [19] T. Murata, K. Shimizu, M. Narita, V. Manganiello, T. Tagawa, Anticancer Res. 22 (2002) 3171–3174.
- [20] T. Murata, T. Sugatani, K. Shimizu, V. Manganiello, T. Tagawa, Anticancer Drugs 12 (2001) 79–83.
- [21] E. Moon, R. Lee, R. Near, L. Weintraub, S. Wolda, A. Lerner, Clin. Cancer Res. 2 (2002) 589–595.
- [22] H. Vainio, H. Moller, Eur. J. Cancer. 29 (1993) 1226–1227.
- [23] J.S. Bertram, Mol. Aspects. Med. 21 (2000) 167–223.
- [24] F. Hadizadeh, S.A. Moallem, M.R. Jaafari, M. Shahab, M. Alahyari, M. Rameshrad, A. Samiei, Chem. Biol. Drug. Des. 73 (2009) 668–673.
- [25] J. Tavakkol-Afshari, A. Brook, S.H. Mousavi, Food Chem. Toxicol. 46 (2008) 3443–3447.